

# Bounding Formulae for the Capacitance of a Cylindrical Two-dimensional Capacitor with Cartesian Orthotropic Dielectric Material

ATTILA BAKSA, ISTVÁN ECSEDI  
Institute of Applied Mechanics,  
University of Miskolc,  
3515 Miskolc-Egyetemváros,  
HUNGARY

*Abstract:* This paper addresses the evaluation of a two-dimensional cylindrical capacitor featuring homogeneous Cartesian anisotropic dielectric material. The development of a bounding formula forms the crux of the investigation and is grounded in the principles of the Cauchy-Schwarz inequality, a mathematical concept widely acknowledged for establishing relationships between different mathematical entities. In the course of this study, a dual-sided bound is systematically derived for the circular cylindrical two-dimensional capacitor through the application of well-established inequality relations. These bounds play a pivotal role in setting limits on the capacitance of the system, providing valuable insights into its electrical behavior.

*Key-Words:* capacitance, orthotropic, hollow circular domain, upper and lower bounds, analytical solution

Received: January 19, 2023. Revised: October 15, 2023. Accepted: November 16, 2023. Published: December 21, 2023.

## 1 Introduction

This paper delves into the intricacies of capacitance analysis, specifically focusing on an infinitely long cylindrical capacitor. The capacitor under consideration is composed of homogeneous Cartesian orthotropic dielectric material. The inequalities presented in this study play a pivotal role in establishing both upper and lower bounds for the capacitance of the unit length of the capacitor.

Capacitance, defined as the ability of a capacitor to store electric charge per unit voltage across its inner and outer surfaces, is a critical parameter influenced by the capacitor's geometry and the permittivity of the dielectric material between its conductor surfaces. Exact capacitance values are known only for capacitors with simplistic shapes. Therefore, the principles and methodologies employed to create upper and lower bounds for the numerical value of capacitance become crucial, as highlighted in references [1], [2], [3], [4], and [5].

In prior work [6] an analytical solution is provided for a spherical capacitor, comparing it with a numerically determined solution achieved through the division of the spherical surface into numerous subregions. Other contributions' calculation of potential distribution for a parallel plate capacitor [7], or an exploration of capacitance determination for regular solids [8], and a provision of error bounds for the capacitance matrix elements in a system of conduction [9], showcase the diverse approaches in the field.

The paper [10] stands out for calculating improved upper and lower bounds for the capacitance of a cube,

employing a combination of the Kelvin inversion and random walk method. A recent work [11] contributes bounding formulae for the capacitance of a cylindrical two-dimensional capacitor with a nonhomogeneous and isotropic dielectric material.

In essence, this paper adds to the body of knowledge by specifically addressing the capacitance of an infinitely long cylindrical capacitor, providing valuable insights into the realm of electrical characteristics influenced by geometric considerations and dielectric material properties. The establishment of bounding formulae contributes to the broader understanding of capacitance estimation, offering a foundation for practical applications and validation of numerical simulations.

In this paper, lower and upper bounds will be derived for the capacitance of a two-dimensional capacitor with homogeneous but Cartesian orthotropic dielectric.

## 2 Governing Equations

Figure 1 visually represents a two-dimensional hollow plane domain denoted as  $A$ . This domain is characterized by an inner boundary curve,  $\partial A_1$ , and an outer boundary curve,  $\partial A_2$ . The Cartesian coordinate system, labeled as  $Oxyz$ , is employed to define the spatial coordinates within this domain. Notably, the origin of the coordinate system is situated as an inner point of the closed curve  $\partial A_1$ .

The unit vectors of the  $Oxyz$  coordinate system are denoted as  $e_x$ ,  $e_y$ , and the position vector of any arbitrary point  $P$  within the domain  $A$  is represented

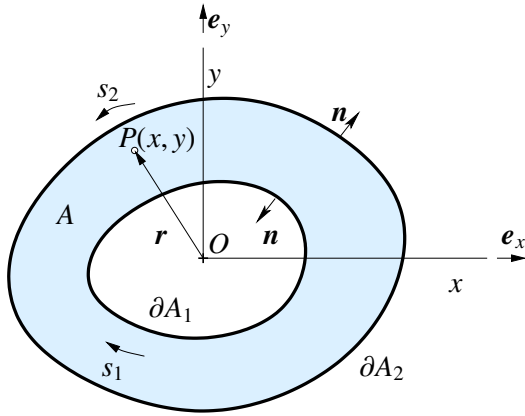


Fig01: Two-dimensional Cartesian orthotropic capacitor.

by  $\mathbf{r} = x\mathbf{e}_x + y\mathbf{e}_y$ . Here,  $x$  and  $y$  are the coordinates of point  $P$  in the  $Oxy$  plane.

It's essential to note that the domain  $A$  is composed of the union of the interior region  $A$  and the boundary  $\partial A$ , where  $\partial A = \partial A_1 \cup \partial A_2$ . This comprehensive description sets the stage for a detailed understanding of the geometric configuration and coordinate system utilized in the subsequent analysis or discussion related to the depicted hollow plane domain.

To give the concept of a capacitor for a two-dimensional hollow domain shown in Figure 1 the following boundary value problem is defined

$$\nabla \cdot (\boldsymbol{\varepsilon} \cdot \nabla U) = 0 \quad \mathbf{r} \in A, \quad (1)$$

$$U(\mathbf{r}) = U_1 \quad \mathbf{r} \in \partial A_1 \quad (2)$$

$$U(\mathbf{r}) = U_2 \quad \mathbf{r} \in \partial A_2 \quad U_1 \neq U_2. \quad (3)$$

Equations (1) and (2) introduce the electric potential, denoted as  $U = U(\mathbf{r})$ , where  $\boldsymbol{\varepsilon}$  represents a two-dimensional positive definite tensor known as the permittivity tensor for the Cartesian anisotropic dielectric material. The operator  $\nabla$  corresponds to the two-dimensional del operator. These expressions are presented within the framework of a Cartesian coordinate system

$$\nabla = \frac{\partial}{\partial x}\mathbf{e}_x + \frac{\partial}{\partial y}\mathbf{e}_y. \quad (4)$$

Equation (1) employs the dot notation to denote the scalar product. The permittivity tensor  $\boldsymbol{\varepsilon}$  finds its matrix representation in equation (5), expressed as

$$\boldsymbol{\varepsilon} = \begin{bmatrix} \varepsilon_1 & 0 \\ 0 & \varepsilon_2 \end{bmatrix} \quad (5)$$

where  $\varepsilon_1 > 0$  and  $\varepsilon_2 > 0$ . Let  $C$  represent the capacitance of the two-dimensional capacitor, measured in

units of [F/m]. The electric energy of the capacitor, [1], [2], [3] and [4], denoted as  $W$ , is given by the expression in equation (6)

$$W = \frac{1}{2}C(U_1 - U_2)^2. \quad (6)$$

To reformulate formula (6), a new function  $u = u(\mathbf{r})$  is introduced. The relationship between  $U = U(\mathbf{r})$  and  $u = u(\mathbf{r})$  is established through equation (7)

$$U(\mathbf{r}) = (U_1 - U_2)u(\mathbf{r}) + U_2. \quad (7)$$

Here,  $u = u(\mathbf{r})$  satisfies the Dirichlet's type boundary-value problem defined by equations (8) and (9).

$$\nabla \cdot (\boldsymbol{\varepsilon}(\mathbf{r}) \cdot \nabla u) = 0 \quad \mathbf{r} \in A, \quad (8)$$

$$u(\mathbf{r}) = 1 \quad \mathbf{r} \in \partial A_1, \quad u(\mathbf{r}) = 0 \quad \mathbf{r} \in \partial A_2. \quad (9)$$

The specific electric energy, [1], [2], [3] and [4], within the dielectric material is computed using equation (10)

$$w = \frac{1}{2}\mathbf{D} \cdot \mathbf{E} = \frac{1}{2}\mathbf{E} \cdot \boldsymbol{\varepsilon} \cdot \mathbf{E} = \frac{1}{2}\nabla U \cdot \boldsymbol{\varepsilon} \cdot \nabla U = \frac{1}{2}(U_1 - U_2)^2 \nabla u \cdot \boldsymbol{\varepsilon} \cdot \nabla u. \quad (10)$$

The overall electric energy of the two-dimensional capacitor denoted as  $W$ , is given by equation (11)

$$W = \int_A w \, dA = \frac{1}{2}(U_1 - U_2)^2 \int_A \nabla u \cdot \boldsymbol{\varepsilon} \cdot \nabla u \, dA. \quad (11)$$

Comparing equation (6) with equation (11) results in an explicit formula for capacitance, as given by equation (12)

$$C = \int_A \nabla u \cdot \boldsymbol{\varepsilon} \cdot \nabla u \, dA. \quad (12)$$

An alternative expression for capacitance  $C$  is derived, commencing with equation (13)

$$0 = u \nabla \cdot (\boldsymbol{\varepsilon} \cdot \nabla u) = \nabla \cdot (u \boldsymbol{\varepsilon} \cdot \nabla u) - \nabla u \cdot \boldsymbol{\varepsilon} \cdot \nabla u. \quad (13)$$

This leads to the derivation of an alternative expression for capacitance, expressed in equation (14)

$$C = \int_A \nabla u \cdot \boldsymbol{\varepsilon} \cdot \nabla u \, dA = \int_{\partial A_1} \mathbf{n} \cdot \boldsymbol{\varepsilon} \cdot \nabla u \, ds. \quad (14)$$

### 3 Upper'Dound for C

*Theorem 1.* Suppose the function  $F = F(\mathbf{r})$  is continuously differentiable throughout  $A \cup \partial A$  and adheres to the boundary conditions outlined in equation (15)

$$F(\mathbf{r}) = 1 \quad \mathbf{r} \in \partial A_1, \quad F(\mathbf{r}) = 0 \quad \mathbf{r} \in \partial A_2, \quad (15)$$

In such a scenario, the inequality relation expressed in equation (16) holds true

$$C \leq C_U = \int_A \nabla F \cdot \boldsymbol{\varepsilon} \cdot \nabla F \, dA. \quad (16)$$

This theorem establishes a connection between the continuously differentiable function  $F$  and the capacitance  $C$ , affirming the validity of the inequality relation in terms of the gradient of  $F$  and the permittivity tensor  $\boldsymbol{\varepsilon}$ .

*Proof.* The foundation for the inequality relation can be traced back to the Cauchy-Schwarz inequality, encapsulated in equation (17)

$$\left( \int_A \nabla F \cdot \boldsymbol{\varepsilon} \cdot \nabla u \, dA \right)^2 \leq \int_A \nabla F \cdot \boldsymbol{\varepsilon} \cdot \nabla F \, dA \int_A \nabla u \cdot \boldsymbol{\varepsilon} \cdot \nabla u \, dA. \quad (17)$$

A straightforward computation yields

$$\int_A \nabla F \cdot \boldsymbol{\varepsilon} \cdot \nabla u \, dA = \int_{\partial A} F \mathbf{n} \cdot \boldsymbol{\varepsilon} \cdot \nabla u \, ds - \int_A F \nabla \cdot (\boldsymbol{\varepsilon} \cdot \nabla u) \, dA = \int_{\partial A_1} \mathbf{n} \cdot \boldsymbol{\varepsilon} \cdot \nabla u \, ds. \quad (18)$$

The combination of inequality (17) with equation (18), along with the utilization of the formula (14), results in the establishment of the upper bound expressed in (16). A concise examination reveals that equality in (16) is only valid if  $F(\mathbf{r}) = u(\mathbf{r})$ . This crucial insight enhances the significance of the derived inequality relation.

### 4 Lower'Dound for C

*Theorem 2.* Consider a vector field  $\mathbf{q} = \mathbf{q}(\mathbf{r})$  defined in the hollow two-dimensional domain  $\bar{A} = A \cup \partial A$ . Suppose  $\mathbf{q}$  satisfies the equation

$$\nabla \cdot (\boldsymbol{\varepsilon} \cdot \mathbf{q}) \quad \mathbf{r} \in A. \quad (19)$$

In this scenario, the following lower-bound formula holds

$$C \geq C_L = \frac{\left( \int_{\partial A_1} \mathbf{n} \cdot \boldsymbol{\varepsilon} \cdot \mathbf{q} \, ds \right)^2}{\int_A \mathbf{q} \cdot \boldsymbol{\varepsilon} \cdot \mathbf{q} \, dA}, \quad \int q^2 \, dV \neq 0. \quad (20)$$

Equality in the lower bound formula (20) is achieved only if

$$\mathbf{q} = \lambda \nabla u, \quad (21)$$

where  $\lambda$  is an arbitrary constant that is different from zero. This result establishes a connection between the vector field  $\mathbf{q}$  and the lower bound capacitance  $C_L$ , providing insight into the conditions under which equality is attained.

*Proof.* The proof of Theorem 2 is based on the following Cauchy-Schwarz inequality relation

$$\left( \int_A \mathbf{p} \cdot \boldsymbol{\varepsilon} \cdot \mathbf{q} \, dA \right)^2 \leq \int_A \mathbf{p} \cdot \boldsymbol{\varepsilon} \cdot \mathbf{p} \, dA \int_A \mathbf{q} \cdot \boldsymbol{\varepsilon} \cdot \mathbf{q} \, dA. \quad (22)$$

Let

$$\mathbf{p} = \nabla u \quad (23)$$

be in (22). A simple calculation yields the result

$$\int_A \nabla u \cdot \boldsymbol{\varepsilon} \cdot \mathbf{q} \, dA = \int_{\partial A} u \mathbf{n} \cdot \boldsymbol{\varepsilon} \cdot \mathbf{q} \, ds - \int_A u \nabla \cdot (\boldsymbol{\varepsilon} \cdot \mathbf{q}) \, dA = \int_{\partial A_1} \mathbf{n} \cdot \boldsymbol{\varepsilon} \cdot \mathbf{q} \, ds. \quad (24)$$

Substitution equation (24) into inequality (22) gives

$$\left( \int_{\partial A_1} \mathbf{n} \cdot \boldsymbol{\varepsilon} \cdot \mathbf{q} \, ds \right)^2 \leq C \int_A \mathbf{q} \cdot \boldsymbol{\varepsilon} \cdot \mathbf{q} \, dA, \quad (25)$$

which shows the validity of Theorem 2.

*Theorem 3.* Consider a non-identically constant function  $f = f(\mathbf{r})$  within the hollow two-dimensional domain  $\bar{A} = A \cup \partial A$ . Assume that  $f$  satisfies the Laplace equation

$$\nabla \cdot \nabla f = \Delta f = 0 \quad \mathbf{r} \in A \cup \partial A. \quad (26)$$

In this context, the following lower bound formula holds for the capacitance  $C$

$$C \geq C_L = \frac{\left( \int_{\partial A_1} \frac{\partial f}{\partial n} \, ds \right)^2}{\int_A \nabla f \cdot \boldsymbol{\varepsilon}^{-1} \cdot \nabla f \, dA}. \quad (27)$$

This lower bound formula establishes a connection between the non-identically constant function  $f$  and

the capacitance  $C$ , shedding light on the lower limits of capacitance under the given conditions.

*Proof.* The verification of the lower bound (27) can be derived from Theorem 2 by considering the vector  $\mathbf{q} = \mathbf{q}(\mathbf{r})$  defined as

$$\mathbf{q}(\mathbf{r}) = \varepsilon^{-1} \cdot \nabla f. \quad (28)$$

In equations (27) and (28),  $\varepsilon^{-1}$  represents the inverse of  $\varepsilon$ , given by

$$\varepsilon^{-1} = \begin{bmatrix} \frac{1}{\varepsilon_x} & 0 \\ 0 & \frac{1}{\varepsilon_y} \end{bmatrix}. \quad (29)$$

This choice of  $\mathbf{q}$  satisfies the conditions of Theorem 2, and by applying it to the theorem's lower bound formula, we establish the validity of the equation (27).

## 5 Geometric Capacitance

The geometric capacitance  $C_0$ , characterizing the two-dimensional hollow domain depicted in Figure 1, is defined as follows

$$C_0 = \int_A \|\nabla u_0\|^2 dA, \quad (30)$$

where  $u_0$  satisfies the Laplace equation

$$\Delta u_0 = 0 \quad \mathbf{r} \in A, \quad (31)$$

with boundary conditions

$$u_0(\mathbf{r}) = 1 \quad \mathbf{r} \in \partial A_1 \quad (32)$$

$$u_0(\mathbf{r}) = 0 \quad \mathbf{r} \in \partial A_2. \quad (33)$$

It is worth noting the validity of the following formula, expressing  $C_0$  in terms of the boundary

$$C_0 = \int_{\partial A_1} \mathbf{n} \cdot \nabla u_0 ds = \int_{\partial A_1} \frac{\partial u_0}{\partial n} ds. \quad (34)$$

By invoking Theorem 1 and Theorem 3, along with equations (30) and (31), it can be inferred that

$$\frac{\int_A \nabla u_0 \cdot \varepsilon \cdot \nabla u_0 dA}{C_0} \geq \frac{C}{C_0} \geq \frac{C_0}{\int_A \nabla u_0 \cdot \varepsilon^{-1} \cdot \nabla u_0 dA}. \quad (35)$$

These inequalities establish a relationship between the capacitance  $C$  and the geometric capacitance  $C_0$ , offering insights into the interplay between the electrical properties of the domain and its geometric characteristics.

## 6 Example. The capacitance of Hollow Circular Domain

The hollow circular domain, depicted in Figure 2, features a cross-section bounded by two concentric circles with inner and outer radii denoted as  $R_1$  and  $R_2$ , respectively. The equations of the boundary circles are given by

$$x^2 + y^2 - R_1^2 = 0 \quad x^2 + y^2 - R_2^2 = 0. \quad (36)$$

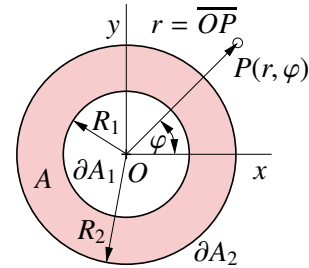


Fig. 2: Two-dimensional hollow circular domain.

Let the function  $F(x, y)$  be defined as

$$F(x, y) = \frac{\ln \frac{x^2 + y^2}{R_2^2}}{\ln \frac{R_1^2}{R_2^2}} \quad (x, y) \in A \cup \partial A \quad (37)$$

Applying the bounding formula (16) for  $F = F(x, y)$  yields

$$C \leq C_U = \frac{\varepsilon_x + \varepsilon_y}{2} \frac{2\pi}{\ln \frac{R_2}{R_1}}. \quad (38)$$

To establish a lower bound for the capacitance using inequality relation (27), the harmonic function (see Figure 2)

$$f(\mathbf{r}) = \ln r^2 = \ln(x^2 + y^2) \quad (39)$$

will be employed. It can be verified that the following equations hold:

$$\frac{\partial f}{\partial x} = \frac{2x}{x^2 + y^2}, \quad \frac{\partial f}{\partial y} = \frac{2y}{x^2 + y^2}, \quad (40)$$

$$\left( \int_{\partial A_1} \frac{\partial f}{\partial n} ds \right)^2 = 16\pi^2, \quad (41)$$

$$\nabla f \cdot \varepsilon^{-1} \cdot \nabla f = \frac{1}{\varepsilon_x} \left( \frac{\partial f}{\partial x} \right)^2 + \frac{1}{\varepsilon_y} \left( \frac{\partial f}{\partial y} \right)^2 = \frac{4}{r^2} \left( \frac{\cos^2 \varphi}{\varepsilon_x} + \frac{\sin^2 \varphi}{\varepsilon_y} \right). \quad (42)$$

Substituting equations (41) and (42) into the lower bound formula (27) leads to the results

$$C > C_L = \frac{2\pi}{\frac{1}{2} \left( \frac{1}{\varepsilon_x} + \frac{1}{\varepsilon_y} \right) \ln \frac{R_2}{R_1}}. \quad (43)$$

These findings establish a relationship between the capacitance  $C$  and the geometric properties of the circular domain, offering valuable insights into its electrical behavior.

Let

$$\varepsilon_x = 8 \times 10^{-12} \frac{\text{F}}{\text{m}}, \quad \varepsilon_y = 9 \times 10^{-12} \frac{\text{F}}{\text{m}}, \quad (44)$$

$$R_1 = 0.015 \text{ m}, \quad R_2 = 0.02 \text{ m} \quad (45)$$

be in the upper and lower bound formulae (38) and (43). In this case, we have

$$1.850\,037\,965 \times 10^{-10} \frac{\text{F}}{\text{m}} \leq C$$

$$C \leq 1.907\,395\,540 \times 10^{-10} \frac{\text{F}}{\text{m}}. \quad (46)$$

We introduce parameter  $\lambda$  according to the following definition

$$\lambda = \frac{R_2}{R_1} > 1. \quad (47)$$

The expressions of  $C_U$  and  $C_L$  as function of  $\lambda$  can be represented as

$$C_U(\lambda) = \frac{\lambda^2 + 1}{\lambda^2 - 1} (\varepsilon_x + \varepsilon_y) \pi, \quad (48)$$

$$C_L(\lambda) = \frac{4\pi\varepsilon_x\varepsilon_y}{(\varepsilon_x + \varepsilon_y) \ln \lambda}. \quad (49)$$

The plots of  $C_U(\lambda)$  and  $C_L(\lambda)$  as a function of  $\lambda$  are shown in Figure 3 for  $1.1 < \lambda \leq 6$ .

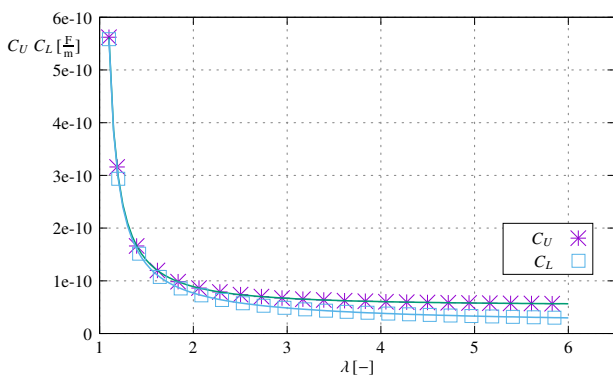


Fig. 3: The plots of  $C_U(\lambda)$  and  $C_L(\lambda)$  as a function of  $\lambda$  for  $1.1 \leq \lambda \leq 6$ .

We note that, from the upper bound formula (16) by the application of following function

$$F(x, y) = \frac{\ln \left( \frac{r}{R_2} \right)^2}{\ln \left( \frac{R_1}{R_2} \right)^2} = \frac{\ln \frac{x^2 + y^2}{R_2^2}}{\ln \left( \frac{R_1}{R_2} \right)^2} \quad (50)$$

we obtain

$$C \leq C_U = \frac{2\pi}{\ln \frac{R_2}{R_1}} \frac{\varepsilon_x + \varepsilon_y}{2}. \quad (51)$$

In the present numerical example the use of formula (51) gives

$$C \leq 1.856\,461\,708 \times 10^{-10} \frac{\text{F}}{\text{m}}. \quad (52)$$

In the case of isotropic dielectric material, the proven upper and lower bounds give the same result.

## 7 Conclusions

This study introduces upper and lower bounds for the capacitance of a two-dimensional capacitor, showcasing a rigorous analysis within the context of homogeneous Cartesian orthotropic dielectric materials. The formulation of these bounds relies on the application of the Cauchy-Schwarz inequality relation, offering a robust foundation for proving the bounding formulae.

By presenting these bounding formulae, the research not only contributes to the theoretical understanding of capacitance in orthotropic dielectric materials but also establishes practical tools for validation. An illustrative example is provided to demonstrate the practical application of the derived upper and lower bounds, offering insights into the real-world implications of the formulated formulas.

These proven bounding formulae hold significance beyond theoretical considerations, providing a valuable means for validating numerical computations. Specifically, these bounds can be utilized to assess and verify results obtained through numerical methods such as the finite element method and other computational solutions. This not only enhances the reliability of numerical simulations but also fosters a deeper understanding of the intricate interplay between material properties and the electrical characteristics of two-dimensional capacitors.

In essence, this research bridges theoretical insights with practical applications, offering a comprehensive exploration of capacitance bounds in the realm of homogeneous Cartesian orthotropic dielectric materials. The developed formulae not only expand our theoretical understanding but also serve as valuable tools for quality assurance in numerical simulations, reinforcing the robustness of computational results in the study of two-dimensional capacitors.

## References

- [1] J.D. Jackson. *Classical Electrodynamics*. Wiley and Sons, New York, 1988.
- [2] L. Solymar. *Lectures on Electromagnetic Theory: a Short Course for Engineers*. Oxford University Press, Oxford, 1984.
- [3] L.D. Landau, L.P. Pitaevskii, E.M. Lifshitz. *Electrodynamics of Continuous Media*. Pergamon Press, Oxford, 1984.
- [4] P. Hammond. *Energy Method in Electromagnetism*. Clarendon Press, Oxford, 1997.
- [5] P.P. Silvester, R.L. Ferrari. *Finite Elements for Electrical Engineers*. Cambridge University Press, 1983.
- [6] E.W. Bai, K.E. Longren. The spherical capacitor a vehicle to introduce numerical methods. *Computer and Electrical Engineering*, 29(1), pp.231–243, 2003.
- [7] D.F. Bartlett, T.R. Corle. The circular parallel plate capacitor: a numerical solution for the potential. *Journal of Physics A: Mathematical and General*, 18(9), pp.1337–1342, 1985.
- [8] W.E. Parr. Upper and lower bounds for the capacitance of regular solids. *Journal of the Society for Industrial and Applied Mathematics*, 19(3), pp.334–386, 1961.
- [9] D.W. Kammler. An error bound for the capacitance calculations. *SIAM, Journal of Numerical Analysis*, 6(2), pp.254–257, 1969
- [10] H.J. Wintle. The capacitance of a cube and square plate by random walk methods. *Journal of Electrostatics*, 62(1), pp.51–62, 2004.
- [11] I. Ecsedi, A.J. Lengyel. Bounding formulae for capacitance of cylindrical capacitor with non-homogeneous dielectric material. *WSEAS Transactions on Electronics*, 12, pp.125–131, 2021.

### **Contribution of Individual Authors to the Creation of a Scientific Article (Ghostwriting Policy)**

István Ecsedi and Attila Baksa carried out the investigation and the formal analysis. István Ecsedi has implemented the algorithm for the example. Attila Baksa was responsible for the validation and for the visualization of the results. All authors have been writing the paper with original draft, review, and editing.

### **Sources of Funding for Research Presented in a Scientific Article or Scientific Article Itself**

The author(s) received no financial support for the research, authorship, and/or publication of this article.

### **Conflicts of Interest**

Furthermore, on behalf of all authors, the corresponding author states that there is no conflict of interest.

### **Creative Commons Attribution License 4.0 (Attribution 4.0 International, CC BY 4.0)**

This article is published under the terms of the Creative Commons Attribution License 4.0  
[https://creativecommons.org/licenses/by/4.0/deed.en\\_US](https://creativecommons.org/licenses/by/4.0/deed.en_US)